Appl Microbiol Biotechnol (2002) 58:157–163
DOI 10.1007/s00253-001-0839-x

ORIGINAL PAPER

A. Peksel · N.V. Torres · J. Liu · G. Juneau
C.P. Kubicek

^{13}C-NMR analysis of glucose metabolism during citric acid production by *Aspergillus niger*

Received: 17 June 2001 / Received revision: 12 September 2001 / Accepted: 14 September 2001 / Published online: 17 November 2001

Abstract The effect of glucose concentration on glycolytic metabolism under conditions of citric acid accumulation by *Aspergillus niger* was studied with ^{13}C-labelled glucose. The results show that during cultivation at high glucose (14%, w/v), most of the label in citric acid is in C-2/C-4, and is thus due to the pyruvate carboxylase reaction. However, a significant portion is also present in C-1/C-5, whose origin is less clear but most likely due to reconsumption of glycerol and erythritol. Formation of trehalose and mannitol is high during the early phase of fermentation and declines thereafter. The early fermentation phase is further characterized by a high rate of anaplerosis from oxaloacetate to pyruvate, which also decreases with time. At low glucose concentrations (2%, w/v), which lead to a significantly reduced citric acid yield and formation rate, labelling of citrate in C-2/C-4 is decreased and C-1/C-5 labelling increased. Growth on 2% glucose is also characterized by an appreciable scrambling of mannitol and considerable backflux from mannitol to trehalose (indicating tight glycolytic control at the fructose-6-phosphate step) and an increased anaplerotic formation of pyruvate from oxaloacetate. These data indicate that cultivation on high sugar concentrations shifts control of glycolysis from fructose-6-phosphate to the glyceraldehyde-3-phosphate dehydrogenase step.

A. Peksel · C.P. Kubicek (✉)
Sektion für Mikrobielle Biochemie,
Institut für Biochemische Technologie und Mikrobiologie,
TU Wien, Getreidemarkt 9/172.5, 1060 Vienna, Austria
e-mail: ckubicek@ mail.zserv.tuwien.ac.at

A. Peksel
Yildiz T. Universitesi, Fen Edebiyat Fak., Kimýa Bölümü,
Biokimya A.B.D., 80270 Sisli, Istanbul, Turkey

N.V. Torres
Grupo de Tecnologia, Bioquimica y Control Metabolico,
Departamento Bioquimica y Biologia Molecular,
Universidad de La Laguna, La Laguna 38206, Tenerife,
Canary Islands, Spain

J. Liu
Soil Plant Dynamics Unit
and Centre for Nonlinear Systems in Biology,
Scottish Crop Research Institute, Dundee DD2, UK

G. Juneau
NMR Analysis and Consulting, 2121 South Imboden Court,
Decatur, IL 62521, USA

Introduction

The metabolic characteristics of citric acid production by *Aspergillus niger* have been the subject of numerous investigations. Today, most of the biochemical steps of glucose metabolism to citric acid have been characterized and/or their genes have been cloned (Kubicek 1998; Wolschek and Kubicek 1998; Ruijter et al. 2002). The results from the above studies were recently used for metabolic modelling and optimization in combination with a mathematical description of the citric acid-producing metabolism, using two different analysis approaches: the biochemical system theory (Alvarez-Vasquez et al. 2000) and the metabolic flux analysis (Guebel and Torres 2001). The validity of these studies, however, is limited by the fact that the relative metabolic flux rates employed for these calculations were based on data from ^{14}C tracer experiments (Cleland and Johnson 1954; Shu et al. 1954). In these studies, the authors resuspended pre-grown, citric acid-producing mycelia of *A. niger* in new medium containing low concentrations of ^{14}C-glucose, a procedure today known to lead to metabolic alterations and a decrease in the rate of citric acid accumulation (Xu et al. 1989). These studies, although considered as pioneering investigations in citric acid accumulation, therefore need critical reassessment.

^{13}C-NMR is powerful alternative to ^{14}C-labelling, as cultivation on high concentrations of ^{13}C-labelled glucose is possible and thus no replacement steps are necessary. We used this technique to investigate how the concentration of the carbon source, which is known to be a crucial parameter for high yields in citric acid fermentation (Shu and Johnson 1948; Xu et al. 1989), influences the metabolic regulation and fluxes of the enzymatic steps from glucose to citrate. We have previously shown

that the positive effect of the sugar concentration is most likely due to its effect on the regulation of glycolysis (Kubicek-Pranz et al. 1990; Arisan-Atac et al. 1996; Alvarez-Vasquez et al. 2000).

Materials and methods

Materials

^{13}C-1-glucose (99% enriched) was purchased from Isotec (Miamisburg, Ohio), and diluted with unlabelled glucose to a final concentration of 10% (w/w) ^{13}C label. Commercially available crystalline food-quality beet sugar (Leopoldsdorfer Zuckerfabrik, Niederösterreich, Austria) was used as a source of sucrose and purchased from local groceries. Stock solutions of both sugars (20%, w/v) were decationized by thrice treating 2 l of the 20% (w/v) solutions for 10 min each with 100 g of Dowex 50WX8. The resulting metal ion-free sugar solutions were stored at –20 °C until use. All other chemicals used were standard analytical grade and provided by local suppliers.

Organisms and cultivation

The organism used was *A. niger* ATCC 11414, a strain producing high yields of citric acid (Shu and Johnson 1947), which is the same strain as that used in earlier tracer studies (Shu and Johnson 1948; Shu et al. 1954). Methods for storage and preparation of conidia for inoculation and cultivation in 1-l, wide-mouthed shake-flasks were as described previously (Xu et al. 1989; Kubicek-Pranz et al. 1990). For ^{13}C-labelled citric acid fermentations, *A. niger* was grown in 1-l, wide-mouthed shake-flasks containing 100 ml of medium (Shu and Johnson (1948) with 14% (w/v) or 2% (w/v) of 10% ^{13}C-labelled glucose as carbon source. All cultivations were checked for high accumulations of citric acid and only those leading to final yields of at least 75 mol% were used for data analysis.

Sample preparation and analysis

Mycelia were separated by suction filtration through a pre-cooled linen cloth and the clear, extracellular broth was immediately frozen. The mycelia were washed once with 5 vols. of ice-cold tapwater and then instantly submerged in liquid nitrogen and ground with a pestle to a fine powder. The powder was subsequently suspended in 10 vols. of 8% (v/v) perchloric acid in 20% (v/v) ethanol, allowed to reach 0–4 °C and homogenized by a motor-driven Potter-Elvehjem homogenizer. The suspension was then centrifuged (10,000 *g*, 4 °C, 10 min) and the debris was again extracted with 6% (w/v) perchloric acid/20% (v/v) ethanol, as described above. After centrifugation (as above), the two supernatants were combined, neutralized with 3 M K_2CO_3 in 40 mM Tris-base and centrifuged (10,000 *g*, 4 °C, 20 min). The supernatants and the extracellular culture fluid were finally lyophilized and kept until NMR analysis.

For NMR measurement, samples were dissolved in D_2O. For intracellular samples, ^{13}C spectra were obtained at a measuring frequency of 100 MHz, using 79° pulses, an acquisition time of 1.2 s, a relaxation delay of 0.3 s and a decoupler power of 2 Khz, Waltz-16 gated on constantly for full nuclear Overhauser effect (NOE). Measurement of extracellular samples, mainly consisting of citric acid only, was performed with a flip angle of 79°, an acquisition time of 1.2 s, a relaxation delay of 17 s and a decoupler power of 2 Khz, Waltz-16 gated off to quench NOE. Both conditions allowed for 96% integral accuracy.

Two rationales were used for isotope enrichment calculations: (1) integral comparison of enriched and non-enriched carbon sites and (2) the use of satellite information from both ^{13}C and ^{1}H. The latter method was particularly used for citric acid analysis.

In integral comparison, enrichment in a single site can be calculated as:

$$S_c/S_u = 1 + 89.3X_i$$

Here, S_c is the integral of the ^{13}C-enriched site, S_u is the integral of the non-enriched site and X_i is the fraction of ^{13}C enrichment. Considering that the natural abundance of ^{13}C is 1.108%, a 10% ^{13}C enrichment would yield S_c/S_u=9.93.

For enrichment in multiple sites, satellite information was used. Thereby the ^{13}C content of any carbon can be expressed as:

$$X_{1a} = S_{1a}/S_t\left[1.01108X_1 + 0.01108\,(n-1)\right]$$

Here, X_{1a} is the total ^{13}C content at carbon position *a*, S_{1a} is the signal intensity of carbon *a*, S_t is the total signal intensity for all carbons in the molecule and *n* is the number of carbon atoms in the molecule.

Biochemical pathways considered and flux calculations

The metabolic pathway information used for in vivo flux determination of citric acid production by *A. niger* is shown in Fig. 1. It includes the glycolytic pathway, the tricarboxylic acid (TCA) cycle, anaplerotic reactions, trehalose metabolism, the mannitol cycle reactions (Singh et al. 1988) and the pyruvate–phosphoenol pyruvate substrate cycle (PYR/PEP cycle). Fluxes through the corresponding reactions were calculated from the ^{13}C label as follows:

1. Mannitol metabolism. Under conditions of an operative mannitol cycle the label in 1-C and 6-C of glucose become scrambled, due to the symmetry of mannitol. Therefore, the operation of mannitol cycle can be assessed by assuming that the C-1 label in trehalose is solely generated from both C-1 in glucose and the labelled C-1 and C-6 in mannitol, while labelled C-6 in trehalose is solely generated from the labelled C-1 and C-6 in mannitol. Therefore:

$$\frac{V_{GLU-TRE}}{V_{MAN-TRE}} = \frac{X^1_{TRE} - 0.5X^1_{MAN}}{1 - X^1_{TRE}} \quad (1)$$

or:

$$\frac{V_{GLU-TRE}}{V_{MAN-TRE}} = \frac{0.5X^1_{MAN} - X^6_{TRE}}{X^6_{TRE}} \quad (2)$$

Here, *X* stands for the fraction of labelled molecules specified by the subscript at a position specified by the superscript in all labelled molecules, *MAN* is mannitol, *TRE* is trehalose and *GLU* is glucose.

2. Anaplerosis of the TCA cycle. PYR is transformed into oxaloacetate (OAA) by a constitutive cytosolic pyruvate carboxylase. The 1,2,3-^{13}C-OAA so formed may then be converted to fumarate by a cytosolic malate dehydrogenase, resulting in the randomization of oxaloacetate carbon to give 4,3,2-^{13}C-OAA.
3. The TCA cycle. 1,2,3-^{13}C-OAA and 4,3,2-^{13}C-OAA condense with unlabelled acetyl-CoA to form citrate (CIT; 6,3,2-^{13}C-CIT and 1,2,3-^{13}C-CIT, respectively). Since aconitase catalyses an equilibrium reaction, the isocitrate dehydrogenase reaction is reversible and ^{13}C-6 of CIT can exchange with unlabelled CO_2. This would decrease the relative enrichment of 6,3,2-^{13}C-CIT that is converted to –,3,2-^{13}C-CIT. Similarly, –,6,3-^{13}C-CIT, –,3,6-^{13}C-CIT and –,–,6-^{13}C-CIT formed after *n* turns of the TCA cycle are converted to –,–,3-^{13}C-CIT, –,3,– -^{13}C-CIT and unlabelled citrate, respectively (Fernandez and Des Rosiers 1995). 6,3,2-^{13}C-CIT and 1,2,3-^{13}C-CIT are decarboxylated to –,3,2-^{13}C-αKG and 1,2,3-^{13}C-αKG. After one cycle, the -ketoglutarate (αKG) is converted to –,3,4-^{13}C-OAA and –,2,1-^{13}C-OAA and their symmetric, inverted pairs: –,4,3-^{13}C-OAA and –,1,2-^{13}C-OAA, respectively. The reaction catalysed by the α-ketoglutarate dehydrogenase is considered to be irreversible (Sheu and Blass 1999). Hence, the second TCA cycle yields –,2,1-^{13}C-CIT, –,3,6-^{13}C-CIT, –,1,2-^{13}C-CIT and –,6,3-^{13}C-

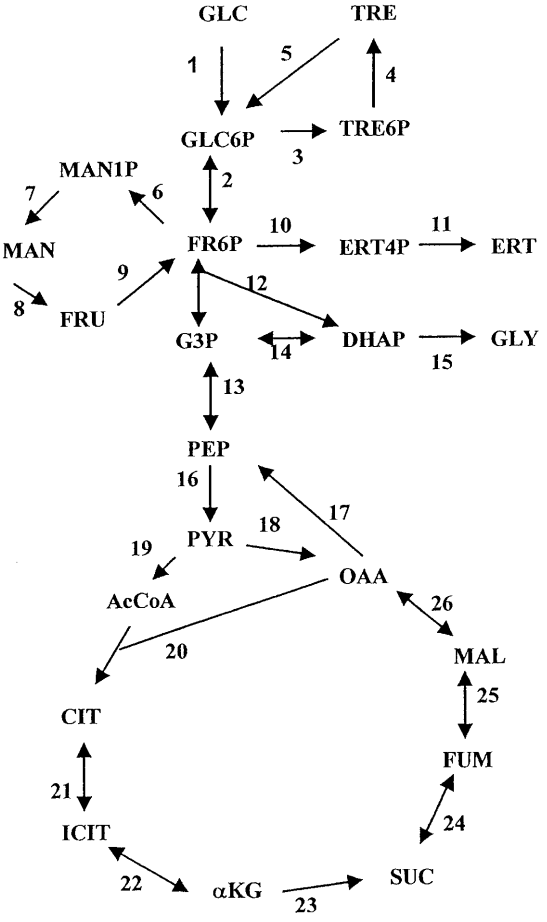

Fig. 1 Metabolic model used for in vivo flux determinations in *Aspergillus niger*. *Double-headed arrows* indicate reversible reactions. Intermediates: *αKG* α-ketoglutarate, *AcCoA* acetyl CoA, *CIT* citrate, *DHAP* dihydroxyacetone phosphate, *ERT* erythritol, *ERT4P* erythrose-4-phosphate, *FRU* fructose, *FRU6P* fructose-6-phosphate, *FUM* fumarate, *G3P* glyceraldehyde-3-phosphate, *GLC* glucose, *GLC6P* glucose-6-phosphate, *GLY* glycerol, *ICT* isocitrate, *MAL* malate, *MAN* mannitol, *MAN1P* mannitol-1-phosphate, *OAA* oxalacetate, *PEP* phosphoenolpyruvate, *PYR* pyruvate, *SUC* succinate, *TRE* trehalose, *TRE6P* trehalose-6-phosphate. Enzymes and metabolic processes: *1* hexokinase/glucokinase system, *2* phosphoglucose isomerase, *3* trehalose-6-phosphate synthase, *4* trehalose-6-phosphate phosphatase, *5* trehalase, *6* mannitol-1-phosphate dehydrogenase, *7* mannitol-1-phosphatase, *8* mannitol dehydrogenase, *9* hexokinase, *10* transketolase, *11* erythritose-4-phosphate phosphatase and erythrose reductase, *12* aldolase, *13* glyceraldehyde-P-dehydrogenase, 3-phosphglycerate kinase, phosphoglycerate mutase and enolase, *14* triose phosphate isomerase, *15* glycerol-3-phosphate dehydrogenase, *16* pyruvate kinase, *17* phosphenolpyruvate carboxykinase, *18* pyruvate carboxylase, *19* pyruvate dehydrogenase, *20* citrate synthase, *21* NAD- and NADP-specific isocitrate dehydrogenase, *23* α-ketoglutarate dehydrogenase, *24* succinyl-CoA synthase and succinate dehydrogenase, *25* fumarase, *26* malate dehydrogenase. Kinetic and physicochemical data were taken from *A. niger* enzymes wherever possible (cf. Wolschek and Kubicek 1998; Ruijter et al. 2002).

CIT, respectively. Finally, pyruvate decarboxylation to acetyl-CoA by pyruvate dehydrogenase forms –,5,4-^{13}C-CIT. After one TCA turn, –,5,4-^{13}C-CIT yields –,1,2-^{13}C-CIT and –,6,3-^{13}C-CIT.

4. Futile cycle PYR/PEP. The OAA formed in the TCA cycle or by the pyruvate carboxylase may enter glycolysis via the PEP-carboxykinase reaction (Woronick and Johnson 1960). The K_{eq} for the PEP-carboxykinase reaction (4.88×10^{-2} atm^{-1}; Woronick and Johnson 1960) suggests that the equilibrium in PEP+ADP+CO_2 → OAA+ATP is on the side of the formation of PEP and is therefore responsible for the randomization of the PYR molecule. The C-5 carbon of CIT (and also of glutamate and α-KG) derives from the C-2 of PYR and therefore this becomes labelled only because of a back reaction from OAA to PYR. Unfortunately, the C-5 carbon of the CIT molecule is spectroscopically indistinguishable from the C-1. Hence, it is not possible to unequivocally attribute the C-1,5 signal of CIT solely to ^{13}C-labelling of the C-1 carbon. However, if no back flux from OAA to PYR takes place, then the C-1 and C-6 carbons of CIT should be equally labelled. Considering that the reaction from OAA to PYR scrambles C-1 and C-6 carbons of CIT to the C-5 carbon via the C-2 in PYR and assuming that labelled OAA is fully scrambled when the reaction OAA to PYR proceeds, we have:

$$\begin{aligned}\frac{d[PYR]^1}{dt} &= V - X^1_{PYR}V_{PYR-OAA} + 0.5X^1_{OAA}V_{OAA-PYR} \\ &\quad + 0.5X^2_{OAA}V_{OAA-PYR} \\ \frac{d[OAA]^1}{dt} &= X^1_{PYR}V_{PYR-OAA} - X^1_{OAA}V_{OAA-PYR} - X^1_{OAA}V.\end{aligned} \tag{3}$$

In these equations, V is the net flux from PYR to OAA for the scrambling of C-1 and C-6 carbons to the C-5 carbon in citrate (V=$V_{PYR-OAA} - V_{OAA-QYR}$). Superscripts stand for the position of the label and subscripts for the compound. $X^a{}_b$ represents the percentage of the labelled molecules at position a in the total labelled molecules considered for compound b. For example, $X^1{}_{PYR}$ is the percentage of PYR molecules labelled at position 1 in all labelled PYR molecules. Unidirectional fluxes are indicated by subscripts. For example, $V_{PYR-OAA}$ is the unidirectional flux from PYR to OAA; and $V_{PYR-OAA}$ stands for the unidirectional flux from PYR to OAA. Similarly, the equations describing the evolution of $[PYR]^2$ and $[OAA]^2$ can be obtained. If we assume that the changes in $[PYR]^1$ and $[OAA]^1$ are sufficiently slow, we have:

$$\frac{V_{OAA-PYR}}{V} = \frac{2X^2_{OAA}}{X^1_{OAA} - X^2_{OAA}} \tag{4}$$

$X^1{}_{OAA}$ and $X^2{}_{OAA}$ can be obtained from the label distribution in citrate. Assuming the average removal rate of C-6 carbon of citrate is $V_{CIT\text{-}C6,}$ then:

$$\begin{aligned}X^2_{OAA} &= \frac{C1,5 - C6 - V_{CIT-C6}t}{C1,5 + C6 + V_{CIT-C6}t} \\ X^1_{OAA} &= 1 - X^2_{OAA}\end{aligned} \tag{5}$$

Results

Incorporation of ^{13}C label into citric acid

In agreement with earlier studies (Xu et al. 1989), growth on 10% (w/v) glucose resulted in a standard type of citric acid fermentation, whereas growth on 2% (w/v) glucose resulted in very low yields of citric acid (Table 1). Based on the time course of these two types of cultivation conditions, samples were taken after 48 h (growth phase), 96 h and 120 h (both idiophase) and after 72 h (late growth phase) and 120 h (idiophase), respectively, and subjected to NMR analysis. Representative examples of ^{1}H spectra of the extracellular culture medium from the cultivation on the high sugar concentration (data not shown) indicated that the major components in the broth were citric acid (pairs of peaks at 2.5–3.0 ppm and peaks between 4.6 ppm and 5.2 ppm)

Table 1 Characteristics of citric acid production on ^{13}C-glucose. Values are means of four different experiments (±SD). Rates were calculated as the average rate at 48–72 h of fermentation in relation to the dry weight at 48 h

Parameters	Glucose concentration (w/v)	
	10%	2%
Citric acid yield (mol mol^{-1})	0.81 (±0.04)	0.12 (±0.02)
Citric acid formation rate (mmol g^{-1} h^{-1}	0.45 (±0.05)	0.057 (±0.011)
Glucose uptake rate (mmol g^{-1} h^{-1})	0.67 (±0.15)	0.15 (±0.07)

Table 2 ^{13}C enrichment of carbons of extracellular citric acid accumulated during growth on 10% and 2% ^{13}C-1-glucose. Values given represent enrichments in single sites (X_i), calculated as described in Materials and methods. Results are from a single experiment only, due to high material costs. However, the data obtained in a second, independent experiment yielded consistent results with respect to relative carbon enrichment and its increase or decrease over the incubation time

Conditions	C-1, 5	C-2, 4	C-3	C-6
10% Glucose				
48 h	0.041	0.070	0.036	0.020
96 h	0.036	0.076	0.036	0.018
120 h	0.032	0.081	0.033	0.018
2% Glucose				
72 h	0.028	0.062	0.049	0.021
96 h	0.033	0.064	0.040	0.017

Table 3 ^{13}C enrichment of carbons of trehalose and mannitol accumulated during growth on 10% and 2% ^{13}C-1-glucose. Values given represent enrichments in single sites (X_i), calculated as described in Materials and methods. Results are from a single experiment only, due to high material costs; however, the data obtained in a second, independent experiment yielded consistent results with respect to relative carbon enrichment and its increase or decrease over the incubation time. *ND* no detectable signal

Conditions		C-1	C-2	C-3	C-4	C-5	C-6
10% Glucose							
Trehalose	72 h	0.095	0.009	0.012	0.012	0.012	0.023
	96 h	0.025	0.002	0.002	0.002	0.002	0.006
	120 h	0.002	ND	ND	ND	ND	ND
Mannitol	72 h	ND	0.014	0.016			
	96 h	ND	0.009	0.007			
	120 h	0.010	0.003	0.003			
2% Glucose							
Trehalose	48 h	0.098	0.008	0.012	0.012	0.011	0.027
	72 h	0.065	0.015	0.013	0.019	0.018	0.037
	96 h	0.063	0.016	0.020	0.018	0.016	0.034
Mannitol	48 h	0.120	0.022	0.023			
	72 h	0.110	0.031	0.031			
	96 h	0.109	0.030	0.030			

and glucose (peaks in the 3.1–4.0 ppm range). Other extracellular components, as detected in earlier studies (Röhr et al. 1987), were below the detection limit of the NMR method and thus were not considered relevant for this study.

Representative examples of ^{13}C-NMR spectra confirmed the appearance of the ^{13}C label in citric acid and glucose exclusively. These analyses were used to follow the distribution of the label or its specific enrichment in the citric acid molecule (Table 2). As can be seen, the ^{13}C label was not localized in one or some of the six carbons of citric acid, but was considerably distributed throughout the molecule. If no scrambling of carbon occurred, the relative intensity of the ^{13}C signal in carbon atoms 1+5, 2+4, 3 and 6 should be 10.9, 2, 1 and 1, respectively (1 indicating natural abundance). In contrast, total scrambling would result in signal ratios of 2:2:1:1. The data presented in Table 2 therefore show that there is considerable scrambling, yet with a clear preference for incorporating the label into C-2 and C-4. During cultivation on high sugar concentrations, the label in C-1, C-5 and C-3 was comparable and C-6 clearly had the least ^{13}C label. Cultivation on the low sugar concentration, in contrast, resulted in an increased label incorporation into C-3 on the expense of C-2, 4. The data also show that the label in atoms 2 and 4 increases with culture time at high sugar concentrations; and this is mainly at the expense of the label in C-1 and C-5, whereas there is little difference in the label of citric acid produced on 2% (w/v) glucose over time.

Incorporation of ^{13}C label into intracellular metabolites

The main intracellular metabolites detected in a ^{13}C-NMR spectrum of intracellular extracts were trehalose, glycerol, erythritol, mannitol and citric acid; and they were detected in mycelia grown on both glucose concentrations. Their appearance in the course of cultivation, however, showed different dynamics and this was also dependent on the concentration of glucose in the medium. During the growth phase on the high sugar concentration, trehalose accumulated earlier and then decreased strongly during idiophase. Mannitol also accumulated early in the growth phase, but its subsequent decrease during idiophase was slower than that of trehalose (Table 3). Glycerol, in contrast, accumulated only during idiophase. Only traces of erythritol were detected and these were not sufficiently resolved to permit label calculations. The abundance of citric acid increased steadily over the incubation period. During growth on the low sugar concentration, all polyols and trehalose were already present during the growth phase and remained at this level throughout the incubation period. The only exception was glycerol, which was not detected in the 120-h sample (Table 4).

The label distribution and specific enrichments in the intracellular metabolites are shown in Table 3. During

Table 4 ^{13}C enrichment of carbons of erythritol and glycerol accumulated during growth on 10% and 2% ^{13}C-1-glucose. Values given represent enrichments in single sites (X_i), calculated as described in Materials and methods. Results are from a single experiment only, due to high material costs; however, the data obtained in a second, independent experiment yielded consistent results with respect to relative carbon enrichment and its increase or decrease over the incubation time. *ND* no detectable signal, – no sample available

Conditions	Time	C1, 4	C2, 3
10% Glucose			
Erythritol	48 h	–	–
	72 h	ND	0.082
	96 h	ND	0.020
	120 h	ND	ND
Glycerol	72 h	ND	ND
	120 h	0.090	0.060
2% Glucose			
Erythritol	48 h	0.100	0.041
	72 h	0.085	0.060
	96 h	0.104	0.043
	120 h	–	–
Glycerol	72 h	0.048	0.015
	120 h	ND	ND

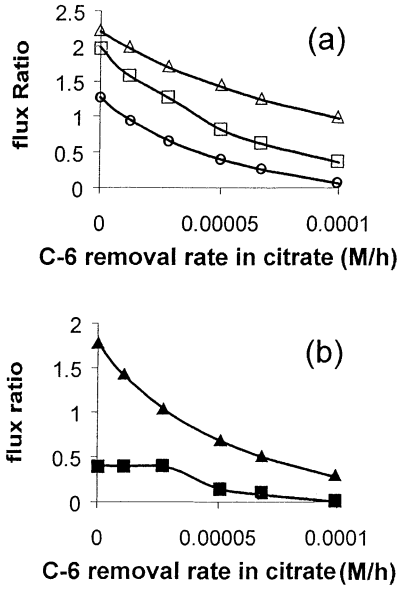

Fig. 2a, b Influence of the sugar concentration on the operation of the pyruvate–phosphoenol pyruvate futile cycle in *A. niger*. The flux ratio is the unidirectional flux from oxalacetate to pyruvate, divided by the flux for generating citrate from oxalacetate. The removal rate of C-6 in citrate is given in arbitrary units (*M*) per hour, showing the dependence of the flux ratio on the C-6 removal rate in citrate. *a* Growth on 10% glucose, *b* growth on 2% glucose. △ 48 h, □ 96 h, ○ 120 h, ■ 72 h, ▲ 96 h (see Materials and methods for details)

growth on high glucose concentrations, the label in trehalose is almost totally unscrambled and 90% of it appears in the C-1 carbon. Carbons 2–5 are completely unlabelled, but some label is present in C-6. This labelling pattern remained constant throughout fermentation. A very similar picture is shown by mannitol, whose label also almost completely appears in C-1/C-6. However, some label is also present in C-3/C-4 and C-2/C-5. Glycerol, in contrast, shows a complete scrambling of label, being theoretically 91% in C-1/C-3 and 120% in C-2. During growth on low sugar concentrations, the label in mannitol was considerably more scrambled and trehalose also contained a higher ^{13}C label in C6, indicating an increased backflux from mannitol to trehalose during growth on low sugar concentrations. The label in erythritol was fully scrambled, whereas most of the label in glycerol occurred in C-1, 3.

Effect of glucose on the fluxes to trehalose and mannitol

The data presented in Table 3 enabled us to calculate the fluxes from glucose to trehalose and mannitol, and between the latter two: on 2% glucose, Eq. 1 estimates that the flux ratio is reduced from 0.53 at 48 h to 0.11 at 72 h and to 0.088 at 96 h, while Eq. 2 shows that the flux ratio is changed from 1.25 at 48 h to 0.45 at 72 h and to 0.60 at 96 h. For 10% glucose, as time increases, Eq. 1 also predicts a reduction in the flux ratio, which is 0.105 at 72 h, 0.026 at 96 h and –0.003 at 120 h (the negative ratio indicates that, at 120 h, the interconversion of glucose and trehalose results in the net loss of labelled C-1 in trehalose). For the data shown in Table 3, it is clear that the C-6 label in trehalose is not due to the reconversion of mannitol at 72 h and 96 h, since no C-1-labelled mannitol is detected at these times. Therefore, it is concluded that, as time increases, the generation of C-1 trehalose from mannitol becomes less important. However, since Eqs. 1 and 2 predict different a flux ratio for 2% glucose and no C-1-labelled mannitol is detected at 72 h and 96 h for 10% glucose, it is clear that other pathways relating to the formation of trehalose also contribute to the randomization of trehalose.

Effect of glucose on the futile cycling between PEP and PYR

Equations 4 and 5, combined with experimental data shown in Table 1, allowed us to test whether the back reaction from OAA to PYR (relative to the formation of CIT from OAA) results in a significant PYR/PEP futile cycle. It can be seen (Fig. 2) that, in the early stages of citrate formation (growth on 10% glucose), the substrate cycle of OAA to PYR is substantial, compared with the flux of OAA to CIT. The relative ratio of the unidirectional flux to PYR versus that of the net flux to CIT then decreases with increasing time. However, for 2% glucose, the opposite finding is obtained. In order to test how this would depend on the TCA activity, the effect of removing C-6 from citrate (due to oxidative decarboxylation by isocitrate dehydrogenase) on the futile cycling between PYR and PEP was also calculated. The data show that an increased rate of C-6 removal from citrate

considerably decreases the operation of the PYR/PEP futile cycle.

Discussion

The highest label from ^{13}C-1-glucose appeared in the C-2/C-4 carbons of citric acid. This finding is in perfect agreement with the operation of pyruvate carboxylase as a major reaction for citric acid accumulation. The increase in ^{13}C label in C-2/C-4 over time is also in accordance with earlier carbon dioxide balances (Kubicek et al. 1979). Furthermore, the finding of lower C-2/C-4 labelling during growth on 2% (w/v) sugar concentrations correlates with a much lower activity of pyruvate carboxylase during growth on low sugar concentrations (Feir and Suzuki 1969). In summary, these data stress the importance of carbon dioxide fixation for citric acid accumulation; and they indicate that sugar concentration is a major factor in determining its in vivo activity.

However, there was also significant label in C-1/C-5 and C-3, whose origin is less obvious. This question is particularly interesting, as the appearance of label in C-1/C-5 was shown to be indirect proportional to that in C-2/C-4. It cannot be due to an operation of the TCA cycle because this would preferentially lead to an enrichment in C-2, 3. It is most likely that this results from a considerable shuttling of trioses and hexoses from glycolysis through the transaldolase and transketolase reactions, as evidenced by the accumulation of glycerol and erythritol. Such a shuttling has recently already been suggested from a metabolic flux balance model (Guebel and Torres 2001). Pyruvate derived from glycerol will be labelled in positions C-1, C-2 and C-3 and will thus introduce label into the C-1 and C-5 of citric acid.

Our data further show that there is a considerable operation of a futile cycle between OAA and PEP during the early phase of citric acid accumulation, which decreases during the later phases of fermentation. Futile cycling at this step has not yet been investigated in filamentous fungi, but has been studied in *Escherichia coli* (Chao and Liao 1994). In that study, the futile cycle was triggered by the overexpression of PEP carboxylase and PEP carboxykinase and resulted in increased glucose and oxygen consumption and excretion of fermentation products. These findings are strikingly similar to the present observations with *A. niger* and suggest that the increased activities of PYR carboxylase during citric acid accumulation may be responsible for this futile cycling. Apparently, the resulting high rate of OAA formation during the early phase of fermentation cannot be used for a similar high rate of CIT formation, which is corroborated by the comparably low portion of carbon dioxide incorporated into CIT during this phase (Kubicek et al. 1979). It is possible that a shortage of NADH (needed to form malate from OAA, which can be transported into the mitochondrion) may be responsible for this during the early phase of citric acid fermentation. Theoretically, catabolism of 1 mol of glucose to pyruvate results in the formation of 2 mol of NADH, of which 1 mol would be needed for the generation of malate. However, this balance is not met when the NADH is used for formation of glycolytic byproducts, such as mannitol (see below) or erythritol (see above).

In accordance with previous studies, there is also a significant accumulation of mannitol (Röhr et al. 1987) and we further show (for the first time) that there is s ignificant accumulation of trehalose. The occurrence of some label in the C-6 of the latter is indicative of a C-1/C-6 equilibration in fructose-6-phosphate by the ction of mannitol-6-phosphate dehydrogenase (Singh et al. 1988), an interpretation which is corroborated by a similar pattern of C-1/C-6 labelling in mannitol. Interestingly, backflux from mannitol to trehalose is strongly increased during growth on low sugar concentrations, as evidenced by considerable introduction of C-6 label from mannitol into trehalose, which indicates a tight glycolytic control at the fructose-6-phosphate step under these conditions.

The absence of scrambling of C-1/C-6 of trehalose (i.e. mannitol formation and backflux) during cultivation on 14% glucose, but its clear presence during cultivation on 2% glucose and the opposite behaviour of glycerol, supports the conclusion that, at the higher sugar concentration, glycolytic control is shifted from the fructose-6-phosphate dehydrogenase step down to that of glyceraldehyde-3-phosphate dehydrogenase. Although earlier findings with *Saccharomyces carlsbergensis* also suggested the existence of control at this step (Jonnalagadda et al. 1982), glyceraldehyde-3-phosphate dehydrogenase is usually not considered to be of regulatory importance. In *A. niger*, this shift of control may be due to the loss of control at the fructose-6-phosphate step during cultivation on high sugar concentrations (Kubicek-Pranz et al. 1990; Wolschek and Kubicek 1998).

In summary, we feel that our study reveals new, detailed insights into sugar catabolism and its relation to citric acid accumulation by *A. niger*, which can be used to design strategies for further improvements in the rate of citric acid production by either traditional or recombinant mutagenesis. In this regard, strains manipulated in the glyceraldehyde-3-phosphate dehydrogenase bottleneck or in the enzymes leading to polyol accumulation would be worth trying.

Acknowledgements This work was supported by a research grant from the Comisión Interministerial de Ciencia y Tecnología from Spain, contract number BIO99-0492-C02-02 and a research grant from Consejería de Educación, Cultura y Deportes del Gobierno de Canarias, ref. PI2000-071, both awarded to N.V.T. N.V.T. would like also to acknowledge the support of the Programa de Acciones Integradas Hispano-Austríacas (HU1998-0009). Financial support for ^{13}C-labelled glucose and NMR analyses to C.P.K.by Tate & Lyle plc, Decatur, Ill., is gratefully acknowledged. The authors are indebted to Drs. J. Lievense and C. Hatzis for their discussions throughout this work. J.L. would like to acknowledge the support of the Scottish Executive Rural Affairs Department and a Royal Society study-visit grant.

References

Alvarez-Vasquez F, González-Alcón C, Torres NV (2000) Metabolism of citric acid production by *Aspergillus niger*: model definition, steady state analysis and constrained optimization of the citric acid production rate. Biotechnol Bioeng 70:82–108

Arisan-Atac I, Wolschek M, Kubicek CP (1996) Trehalose-6-phosphate synthase A affects citrate accumulation by *Aspergillus niger* under conditions of high glycolytic flux. FEMS Microbiol Lett 140:77–83

Chao YP, Liao JC (1994) Metabolic responses to substrate futile cycling in *Escherichia coli*. J Biol Chem 269:5122–5126

Cleland WW, Johnson MJ (1954) Tracer experiments on the mechanism of citric acid formation by *Aspergillus niger*. J Biol Chem 208:679–689

Feir HA, Suzuki I (1969) Pyruvate carboxylase of *Aspergillus niger*: kinetic study of a biotin-containing enzyme. Can J Biochem 47:697–710

Fernandez CA, Des Rosiers C (1995) Modelling of liver citric acid and gluconeogenesis based on ^{13}C mass isotopomer distribution analysis of intermediates. J Biol Chem 270:10037–10042

Guebel D, Torres NV (2001) Optimization of the citric acid production by *Aspergillus niger* through a metabolic flux balance model. Electron J Biotechnol 4:1–17

Jonnalagadda SB, Becker JU, Sel'kov EE, Betz A (1982) Flux regulation in glycogen-induced oscillatory glycolysis in cell-free extracts of *Saccharomyces carlsbergensis*. Biosystems 15:49–58

Kubicek CP, Zehentgruber O, Röhr M (1979) An indirect method for studying fine control of citric acid accumulation by *Aspergillus niger*. Biotechnol Lett 1:47–52

Kubicek CP (1998) Production of citric acid. In: Nagodawithana T, Reed G (eds) Commercial fermentations and nutritional needs of their micro-organism. Esteekay Associates, Milwaukee, pp 236–257

Kubicek-Pranz EM, Mozelt M, Röhr M, Kubicek CP (1990) Changes in the concentration of fructose-2,6-bisphosphate in *Aspergillus niger* during stimulation of acidogenesis by elevated sucrose concentrations. Biochim Biophys Acta 1033:250–255

Röhr M, Kubicek CP, Zehentgruber O, Orthofer R (1987) Accumulation and partial reconsumption of polyols during citric acid fermentation by *Aspergillus niger*. Appl Microbiol Biotechnol 27:235–239

Ruijter GJG, Kubicek CP, Visser J (2002) Production of organic acids by fungi. In: H.D. Osiewacz (ed) The Mycota, vol 10. Industrial applications. Springer, Berlin Heidelberg New York, pp 213–230

Sheu KF, Blass JP (1999) The α-ketoglutarate dehydrogenase complex. Ann NY Acad Sci 893:61–78

Shu P, Johnson MJ (1947) Effect of the composition of the sporulation medium on citric acid production by *Aspergillus niger* in submerged culture. J Bacteriol 54:161–167

Shu P, Johnson MJ (1948) Citric acid production by submerged fermentation with *Aspergillus niger*. Ind Eng Chem 40:1202–1205

Shu P, Funk A, Neish AC (1954) Mechanism of citric acid formation from glucose by *Aspergillus niger*. Can J Biochem 32:68–75

Singh M, Scrutton NS, Scrutton MC (1988) NADPH generation in *Aspergillus nidulans*: is the mannitol cycle involved? J Gen Microbiol 134:643–654

Wolschek MF, Kubicek CP (1998) Biochemistry of citric acid accumulation in *Aspergillus niger*. In: Kristiansen B, Mattey M, Linden J (eds) Citric acid biotechnology. Taylor and Francis, London, pp 11–32

Woronick C, Johnson MJ (1960) Carbon dioxide fixation by cell-free extracts of *Aspergillus niger*. J Biol Chem 235:9–15

Xu DB, Madrid CP, Röhr M, Kubicek CP (1989) Influence of type and concentration of the carbon source on citric acid production by *Aspergillus niger*. Appl Microbiol Biotechnol 30:553–558